Giant magnetoresistance in nanoscale ferromagnetic heterocontacts

2007 J. Phys.: Condens. Matter 19 196215

(http://iopscience.iop.org/0953-8984/19/19/196215)

IOP PUBLISHING JOURNAL OF PHYSICS: CONDENSED MATTER

J. Phys.: Condens. Matter **19** (2007) 196215 (10pp) doi:10.1088/0953-8984/19/19/196215

Giant magnetoresistance in nanoscale ferromagnetic heterocontacts

A N Useinov[1,2], R G Deminov[1], L R Tagirov[1,2] and G Pan[2,3]

[1] Kazan State University, 420008 Kazan, Russian Federation
[2] CRIST, University of Plymouth, Plymouth, Devon PL4 8AA, UK

E-mail: G.Pan@plymouth.ac.uk

Received 29 January 2007
Published 19 April 2007
Online at stacks.iop.org/JPhysCM/19/196215

Abstract

A quasi-classical theory of giant magnetoresistance (GMR) in nanoscale point contacts between different ferromagnetic metals is developed. The contacts were sorted by three types of mutual positions of the conduction spin-subband bottoms which are shifted one against another by the exchange interaction. A model of a linear domain wall has been used to account for the finite contact length. The magnetoresistance is plotted against the size of the nanocontact. In heterocontacts the magnetoresistance effect not only turns out to be negative, as usual, but it can be positive as well. The relevance of the results to existing experiments on GMR in point heterocontacts is discussed.

1. Introduction

The experimental discovery of ultra-high magnetoresistance (MR) in ferromagnetic nanocontacts has attracted considerable attention due to its potential technological applications for future generations of magnetoresistive sensors [1–8]. Two mechanisms of giant magnetoresistance (GMR) in magnetic nanocontacts were proposed to explain the experimental data: one is the enhancement of the impurity scattering in a domain wall (DW) [2, 4], and the other is the scattering of electrons by an energy landscape of DW (domain wall scattering) [9–11]. Both mechanisms essentially exploit the sharpness of the domain wall profile shrinking into a narrow constriction (ultimately of atomic size) [12–15]. The DW scattering theory [11] is general enough to admit spin asymmetry of the bulk impurity scattering (conduction electron mean free path in the spin-subbands of a ferromagnet may differ by five to seven times [16]) as well as the spin asymmetry of the interface scattering (contacting ferromagnets can be different—ferromagnetic heterocontacts). The aim of the present paper is to analyse the influence of the spin-asymmetry of the interface scattering on the magnetoresistance of ferromagnetic point heterocontacts and to search for the optimal conditions at which the GMR effect can be maximized.

[3] Author to whom any correspondence should be addressed.

2. Conductance of a ferromagnetic heterocontact

We consider a small-area contact between two single-domain ferromagnetic metals. When the magnetization on both sides of the contact is in parallel (P) alignment there is no domain wall in the constriction, and the electric current flows through the point contact independently in each of the conduction electron spin-subbands. In an antiparallel (AP) alignment of the magnetizations, a domain wall is created in the constriction [12–15]. Simultaneously, the conduction spin-subband assignment in one of the magnetic domains reverses with respect to the previous one. In the case of a ferromagnetic heterocontact, the band structures of the spin-subbands of the ferromagnetic metals do not coincide with either spin-up or spin-down conduction electrons. It is obvious that the potential barriers at the interface of the contact (see figure insets below) are different for the P and AP alignments. As a result, scatterings of electrons associated with these potential barriers and magnetization profiles at the interface are different for the two alignments, which gives rise to magnetoresistance.

The case of a ferromagnetic homocontact (a contact made of the same ferromagnetic metal) was considered in [11] in the quasi-classical approximation. Using the same approach, here we give a general derivation of the conductance of a ferromagnetic heterocontact made of different ferromagnetic metals. The model of the nanocontact that we consider is a circular hole of radius a made in an impenetrable membrane, which divides the space into two halves, each of which is occupied by a single-domain ferromagnetic metal. The z-axis of the coordinate system is chosen to be perpendicular to the membrane plane. Our aim is to calculate the electric current I^z through the hole in response to the voltage drop V applied to the outer leads far away from the contact:

$$I^z(z \to 0) = a \int_0^\infty \mathrm{d}k\, J_1(ka)\, j^z(0, k). \tag{1}$$

Here the Bessel function $J_1(x)$ comes from the integration of the current density $j^z(z = 0, \boldsymbol{\rho})$ over the contact cross-section, and $j^z(0, k)$ is the Fourier transform of the current density $j^z(z = 0, \boldsymbol{\rho})$ over the in-plane coordinate $\boldsymbol{\rho}$. The current density can be expressed via the antisymmetric quasi-classical Green function (GF), $g_\mathrm{a}(z, \boldsymbol{\rho})$, as follows ($c = \hbar = 1$):

$$j^z(z, \boldsymbol{\rho}) = -\frac{ep_\mathrm{F}^2}{2\pi} \int_0^{\pi/2} \mathrm{d}\Omega_\theta \cos\theta\, g_\mathrm{a}(z, \boldsymbol{\rho}). \tag{2}$$

The antisymmetric GF itself is a solution of the system of Boltzmann-type equations [17]:

$$\begin{aligned} l_{z,\alpha} \frac{\partial g_{\mathrm{a},\alpha}}{\partial z} + \mathbf{l}_{\parallel,\alpha} \frac{\partial g_{\mathrm{s},\alpha}}{\partial \boldsymbol{\rho}} + g_{\mathrm{s},\alpha} - \langle g_{\mathrm{s},\alpha} \rangle = 0, \\ l_{z,\alpha} \frac{\partial g_{\mathrm{s},\alpha}}{\partial z} + \mathbf{l}_{\parallel,\alpha} \frac{\partial g_{\mathrm{a},\alpha}}{\partial \boldsymbol{\rho}} + g_{\mathrm{a},\alpha} = 0, \end{aligned} \tag{3}$$

supplied with the boundary conditions (BC) at interfaces

$$g_{\mathrm{aL},\alpha} = g_{\mathrm{aR},\alpha} = \begin{cases} g_{\mathrm{a},\alpha}, & p_\parallel < p_\mathrm{FL}, p_\mathrm{FR} \\ 0, & \min(p_\mathrm{FL}, p_\mathrm{FR}) < p_\parallel, \end{cases} \tag{4}$$

$$2R_\alpha g_{\mathrm{a},\alpha} = D_\alpha (g_{\mathrm{sL},\alpha} - g_{\mathrm{sR},\alpha}). \tag{5}$$

In the above equations, $g_{\mathrm{s}(a)} = 1/2[g_\alpha(n_z, z, \boldsymbol{\rho}) \pm g_\alpha(-n_z, z, \rho)]$ is the single-particle quasi-classical Green function that is symmetric (antisymmetric) with respect to the projection $n_z = p_{z,\alpha}/p_{\mathrm{F},\alpha}$ of the Fermi momentum $p_{\mathrm{F},\alpha}$ on the axis z; $l_{z,\alpha} = l_\alpha \cos\theta$ is the projection of the spin-dependent electron mean free path l_α on the axis z, $l_{\parallel,\alpha}^2 = l_\alpha^2 - l_{z,\alpha}^2$; $\alpha = (\uparrow, \downarrow)$ is the spin index, and $\boldsymbol{\rho} = (x, y)$ is the coordinate in the plane of the contact. The angular brackets in

$\langle g_s \rangle$ mean averaging over the solid angle: $\langle g_s \rangle = \oint \mathrm{d}\Omega/2\pi \; g_s$, $p_\parallel$ is the projection of the spin-dependent Fermi momentum $p_{F,\alpha}$ on the plane of the contact, and D_α and $R_\alpha = 1 - D_\alpha$ are the angular- and spin-dependent quantum-mechanical transmission and reflection coefficients, respectively. Boundary conditions (4) and (5) obey the specular reflection law:

$$p_\parallel = p_{\mathrm{FL}} \sin\theta_L = p_{\mathrm{FR}} \sin\theta_R. \tag{6}$$

The system of equation (3) can be solved in a mixed representation [11], real-space for the variable z, and Fourier-transformed over the variable $\boldsymbol{\rho}$. The formal solution reads:

$$f_{\mathrm{sL}}(z<0) = -g_{\mathrm{aL}} + \frac{1}{l_{zL}} \int_{-\infty}^{z} \mathrm{e}^{-\kappa_L (z-\xi)} \, \langle f_{\mathrm{sL}}(\xi) \rangle_{\theta_L} \, \mathrm{d}\xi, \tag{7}$$

$$f_{\mathrm{sR}}(z>0) = g_{\mathrm{aR}} + \frac{1}{l_{zR}} \int_{z}^{\infty} \mathrm{e}^{-\kappa_R (\xi - z)} \, \langle f_{\mathrm{sR}}(\xi) \rangle_{\theta_R} \, \mathrm{d}\xi, \tag{8}$$

where $f_s(\varepsilon) = g_s(\varepsilon) - 2\tanh\frac{\varepsilon}{2T}$, $\kappa_i = [1 - \mathrm{i}(\mathbf{k}\mathbf{l}_{i\parallel})]/l_{zi}$. We omit the common spin label to discharge a bit of the complexity of the notation. The above solution allows mean free paths as well as Fermi momenta to be non-equivalent in the contacting ferromagnets. To get the antisymmetric GF, g_a, in a closed form from the solution (7) and (8), we average it over a solid angle at each half-space:

$$\langle f_{\mathrm{sL}}(z<0) \rangle_{\theta_L} = -\langle g_{\mathrm{aL}} \rangle_{\theta_L} + \int_{-\infty}^{z} \left\langle \frac{\mathrm{e}^{-\kappa_L (z-\xi)}}{l_{zL}} \langle f_{\mathrm{sL}}(\xi) \rangle_{\theta_L} \right\rangle_{\theta_L} \mathrm{d}\xi, \tag{9}$$

$$\langle f_{\mathrm{sR}}(z>0) \rangle_{\theta_R} = \langle g_{\mathrm{aR}} \rangle_{\theta_R} + \int_{z}^{\infty} \left\langle \frac{\mathrm{e}^{-\kappa_R (\xi - z)}}{l_{zR}} \langle f_{\mathrm{sR}}(\xi) \rangle_{\theta_R} \right\rangle_{\theta_R} \mathrm{d}\xi. \tag{10}$$

Then, we take the slowly varying symmetric GFs, $\langle f_{\mathrm{sL}}(\xi) \rangle_{\theta_L}$ and $\langle f_{\mathrm{sR}}(\xi) \rangle_{\theta_R}$, out of the integrals in equations (9) and (10) in the point $\xi = z$. The resulting linear equations provide approximate expressions for the angular-averaged symmetric GFs:

$$\langle f_{si}(z) \rangle_{\theta_i} = \mathrm{sgn}(z) \frac{\langle g_{ai} \rangle_{\theta_i}}{1 - \lambda_i}, \tag{11}$$

where

$$\lambda_i = \int_0^\infty \left\langle \frac{\mathrm{e}^{-\kappa_i \eta}}{l_{zi}} \right\rangle_{\theta_i} \mathrm{d}\eta = \frac{1}{k l_i} \arctan(k l_i). \tag{12}$$

Now, solution (11) can be used in combination with equations (7) and (8) to satisfy the boundary condition equation (5). Consecutive substitution of equation (11) into equations (7) and (8), and then the result into BC (5), gives:

$$\begin{aligned} 2g_{\mathrm{a}} = -2D \left[\tanh\left(\frac{\varepsilon}{2T}\right) - \tanh\left(\frac{\varepsilon - eV}{2T}\right) \right] \gamma_k \\ - \frac{\langle g_{\mathrm{aL}} \rangle_{\theta_L}}{1 - \lambda_L} \int_0^\infty D \frac{\mathrm{e}^{-\kappa_L \eta}}{l_{zL}} \mathrm{d}\eta - \frac{\langle g_{\mathrm{aR}} \rangle_{\theta_R}}{1 - \lambda_R} \int_0^\infty D \frac{\mathrm{e}^{-\kappa_R \eta}}{l_{zR}} \mathrm{d}\eta, \end{aligned} \tag{13}$$

where

$$\gamma_k = \int_0^a \mathrm{d}\rho \int_0^{2\pi} \rho \mathrm{e}^{\mathrm{i}\mathbf{k}\rho} \, \mathrm{d}\varphi = \frac{2\pi a}{k} J_1(ka). \tag{14}$$

Assuming first that the antisymmetric GF, g_a, in the left-hand side of (13) is equal to g_{a1}, according to BC (4), and then to g_{a2}, after solid-angle averaging in an appropriate half-space,

we arrive at a system of two equations, the solution of which looks a bit cumbersome:

$$\langle g_{\mathrm{aL}}\rangle_{\theta_L} = -2\left[\tanh\left(\frac{\varepsilon}{2T}\right) - \tanh\left(\frac{\varepsilon - eV}{2T}\right)\right]\gamma_k \times \left\{\langle D\rangle_{\theta_L}\left[2(1-\lambda_L)(1-\lambda_R) + \widetilde{\lambda}_2(1-\lambda_L)\right] - \langle D\rangle_{\theta_R}\widetilde{\lambda}_4(1-\lambda_L)\right\}\mathrm{Den}^{-1}(k), \tag{15}$$

$$\langle g_{\mathrm{aR}}\rangle_{\theta_R} = -2\left[\tanh\left(\frac{\varepsilon}{2T}\right) - \tanh\left(\frac{\varepsilon - eV}{2T}\right)\right]\gamma_k \times \left\{\langle D\rangle_{\theta_R}\left[2(1-\lambda_L)(1-\lambda_R) + \widetilde{\lambda}_1(1-\lambda_R)\right] - \langle D\rangle_{\theta_L}\widetilde{\lambda}_3(1-\lambda_R)\right\}\mathrm{Den}^{-1}(k), \tag{16}$$

where

$$\mathrm{Den}(k) = 4(1-\lambda_L)(1-\lambda_R) + 2\left[\widetilde{\lambda}_1(1-\lambda_R) + \widetilde{\lambda}_2(1-\lambda_L)\right] - \widetilde{\lambda}_4\widetilde{\lambda}_3 + \widetilde{\lambda}_1\widetilde{\lambda}_2, \tag{17}$$

$$\widetilde{\lambda}_1 = \int_0^\infty \left\langle D\frac{\mathrm{e}^{-\kappa_L\eta}}{l_{zL}}\right\rangle_{\theta_L}\mathrm{d}\eta \equiv \langle I_L\rangle_{\theta_L}, \tag{18}$$

$$\widetilde{\lambda}_2 = \langle I_R\rangle_{\theta_R}, \qquad \widetilde{\lambda}_3 = \langle I_L\rangle_{\theta_R}, \qquad \widetilde{\lambda}_4 = \langle I_R\rangle_{\theta_L}. \tag{19}$$

Being substituted into the right-hand side of equation (13), equations (15) and (16) solve the problem of finding the current density, equation (2), and eventually the net current I^z (1) through the nanocontact as follows (a linear approximation on the applied bias voltage V has been utilized):

$$I^z(z\to 0, t=0) = \frac{e^2 p_{\mathrm{F}_L}^2 \pi a^2 V}{\pi^2}\int_0^\infty \mathrm{d}k\,\frac{J_1^2(ka)}{k}F(k), \tag{20}$$

where

$$F(k) = \langle x_L D\rangle_{\theta_L} - \left(G_1\langle x_L I_L\rangle_{\theta_L} + G_2\langle x_L I_R\rangle_{\theta_L}\right), \tag{21}$$

$$G_1 = \left\{\langle D\rangle_{\theta_L}\left[2(1-\lambda_R) + \widetilde{\lambda}_2\right] - \langle D\rangle_{\theta_R}\widetilde{\lambda}_4\right\}\mathrm{Den}^{-1}(k), \tag{22}$$

$$G_2 = \left\{\langle D\rangle_{\theta_R}\left[2(1-\lambda_L) + \widetilde{\lambda}_1\right] - \langle D\rangle_{\theta_L}\widetilde{\lambda}_3\right\}\mathrm{Den}^{-1}(k), \tag{23}$$

$$\langle x_L I_L\rangle_{\theta_L} = \int_0^\infty \left\langle \cos\theta_L D\frac{\mathrm{e}^{-\kappa_L\eta}}{l_{zL}}\right\rangle_{\theta_L}\mathrm{d}\eta, \qquad \langle x_L I_R\rangle_{\theta_L} = \int_0^\infty \left\langle \cos\theta_L D\frac{\mathrm{e}^{-\kappa_R\eta}}{l_{zR}}\right\rangle_{\theta_L}\mathrm{d}\eta. \tag{24}$$

Notice finally that the current given by equation (20) refers to a particular spin-channel of conductance, in spite of the spin index being omitted for brevity. The total current through the nanocontact is the sum of currents for both the spin-channels. The formal expression for the second one is the same, but with all physical parameters referred to the second spin-channel (see section 3).

3. Magnetoresistance of ferromagnetic nanocontacts

3.1. General considerations

The total current through a magnetic nanocontact combines two spin-channels whose conductances are different for P and AP mutual orientations of magnetizations in the banks. The magnetoresistance is characterized by a dimensionless ratio:

$$\mathrm{MR} = \frac{\sigma^{\mathrm{P}} - \sigma^{\mathrm{AP}}}{\sigma^{\mathrm{AP}}}, \tag{25}$$

where $\sigma^{\mathrm{P(AP)}} = \sigma_{\uparrow}^{\mathrm{P(AP)}} + \sigma_{\downarrow}^{\mathrm{P(AP)}}$ ($I^{\mathrm{P(AP)}} = \sigma^{\mathrm{P(AP)}} V$). Then, MR is positive if the physical effect itself is negative (the resistance drops when a magnetic field is applied). Now the dependence of MR on the conduction band parameters of contacting ferromagnets can be analysed.

To account for a finite nanocontact length, we place linear-profile DW inside the nanocontact for the AP alignment of magnetizations [12, 18–20]. The quantum-mechanical transmission coefficient through the linear DW can be expressed as follows:

$$D^{SL}(x, w) = \frac{4k_{\mathrm{M}}k_{\mathrm{m}}t^2(w)\pi^{-2}}{(k_{\mathrm{M}}\boldsymbol{\beta} - k_{\mathrm{m}}\boldsymbol{\gamma})^2 + (k_{\mathrm{M}}k_{\mathrm{m}}\boldsymbol{\alpha} + \boldsymbol{\kappa})^2}, \tag{26}$$

where

$$\begin{aligned}
\boldsymbol{\alpha} &= \mathrm{Ai}\,(q_1 w)\,\mathrm{Bi}\,(q_2 w) - \mathrm{Bi}\,(q_1 w)\,\mathrm{Ai}\,(q_2 w)\,,\\
\boldsymbol{\beta} &= t(w)\left\{\mathrm{Ai}\,(q_1 w)\,\mathrm{Bi}'\,(q_2 w) - \mathrm{Bi}\,(q_1 w)\,\mathrm{Ai}'\,(q_2 w)\right\},\\
\boldsymbol{\gamma} &= t(w)\left\{\mathrm{Ai}'\,(q_1 w)\,\mathrm{Bi}\,(q_2 w) - \mathrm{Bi}'\,(q_1 w)\,\mathrm{Ai}\,(q_2 w)\right\},\\
\boldsymbol{\kappa} &= t^2(w)\left\{\mathrm{Ai}'\,(q_1 w)\,\mathrm{Bi}'\,(q_2 w) - \mathrm{Bi}'\,(q_1 w)\,\mathrm{Ai}'\,(q_2 w)\right\},
\end{aligned} \tag{27}$$

and $t(w) = [2mE_{\mathrm{ex}}/w]^{1/3}$, $E_{\mathrm{ex}} = (k_{\mathrm{FM}}^2 - k_{\mathrm{Fm}}^2)/2m$, $q_1 = -k_{\mathrm{FM}}^2 t(w)/2mE_{\mathrm{ex}}$, and $q_2 = -k_{\mathrm{Fm}}^2 t(w)/2mE_{\mathrm{ex}}$, where w is the half-width of DW; $\mathrm{Ai}(z)$, $\mathrm{Bi}(z)$, $\mathrm{Ai}'(z)$, and $\mathrm{Bi}'(z)$ are the Airy functions and their derivatives; and $k_{\mathrm{m}} = k_{\mathrm{Fm}}\cos(\theta_{\mathrm{m}})$ and $k_{\mathrm{M}} = k_{\mathrm{FM}}\cos(\theta_{\mathrm{M}})$ are the normal components of the wavevector of minority and majority subbands, respectively. Note here that k_{m} is used for a subband with smaller Fermi momentum, and k_{M} for a subband with larger Fermi momentum, whatever the spin projection of the subband, or the side of the contact (left or right), is. The quantum-mechanics textbook expression for the coefficient of transmission through a step-like DW (band-offset model), $D^{\mathrm{step}}(x) = 4k_{\mathrm{M}}k_{\mathrm{m}}/(k_{\mathrm{M}} + k_{\mathrm{m}})^2$, can be retrieved from equation (27) in the limit of $w \to 0$. Again, we omit the spin index to simplify the appearance of the formulas above.

Ferromagnetic heterocontacts mean that the contacting ferromagnets have different parameters for their conduction bands. In our calculations we fix parameters of the ferromagnetic metal at the left bank of the contact (the values $k_{\mathrm{F}\downarrow} = 4\ \mathrm{nm}^{-1}$, $k_{\mathrm{F}\uparrow} = 10\ \mathrm{nm}^{-1}$, and $k_{\mathrm{F}\downarrow}/k_{\mathrm{F}\uparrow} = 0.4$ are close to that for iron cited in [21, 22]), and vary the conduction band properties of the second ferromagnetic metal. Before we proceed with particular calculations, we have to mention an important detail which distinguishes the ferromagnetic heterocontacts from homocontacts. For a parallel configuration of magnetizations in a homocontact, there is no DW in the constricted area, and an electron of either spin-projection moves in a flat potential landscape because materials (conduction bands) on both sides of the contact are identical. Then, the quantum-mechanical transmission coefficient D in both conduction spin-channels is equal to one. In contrast, in a ferromagnetic heterocontact there is always a potential barrier at the nanocontact because the conduction band bottoms do not coincide for either spin projection and magnetization alignments. The only difference is that in the P magnetization configuration there is no DW in the nanocontact, but in the AP configuration there is. Then, for the P alignment we have to assume a sharp change in the band parameters just at the interface of two ferromagnets, but for the AP alignment we place a linear profile DW inside the nanocontact. In a common stream of numerical calculation we simply simulate the sharp interface in the P configuration by a linear DW of about one angström in thickness ($L = 2w = 0.1$ nm).

3.2. Magnetoresistance of a ferromagnetic heterocontact

In a simple parabolic band that we use here, the heterocontacts are sorted by the mutual positions of the bottoms of their conduction spin-subbands in the parallel alignment of magnetizations. Three physically distinct combinations can be considered (see insets in the

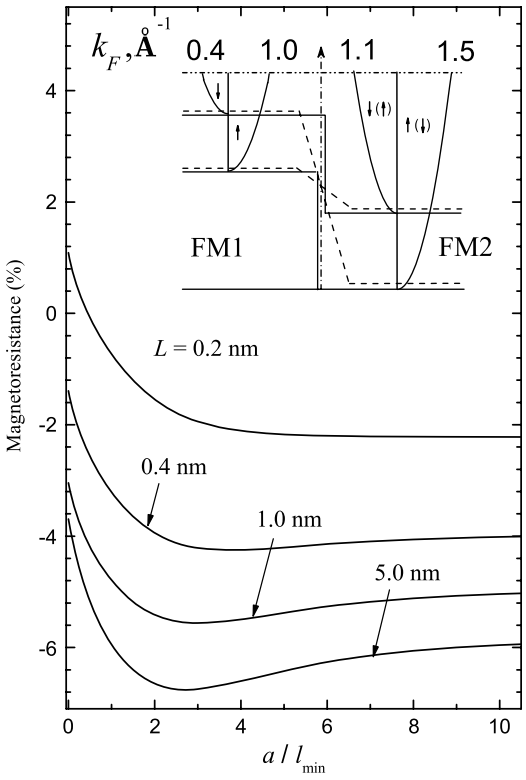

Figure 1. Dependence of MR on the contact size for the case $k_{FL\downarrow} < k_{FL\uparrow} < k_{FR\downarrow} < k_{FR\uparrow}$. The Fermi momenta of the contacting ferromagnets are indicated in the inset; the ratio $l_{L\downarrow}/l_{L\uparrow} = 2$ is taken to be equal to $l_{R\downarrow}/l_{R\uparrow}$ to simplify appearance, and $l_{L\downarrow}/l_{R\downarrow} = 1$.

figures below), and MR for every combination is calculated as a function of the contact size. Looking through the insets of the figures, one may see that the Fermi momentum of a spin-subband from the left to the contact can be larger as well as smaller than that from the right. However, according to the momentum conservation law, equation (6), not every incident angle from the side of the larger momentum is allowed for an electron to transmit to the side of the smaller Fermi momentum. Then, the integrals in equations (18), (19) and (24) can be evaluated as follows:

$$\langle D\rangle_{\theta_L} = \int_{x_c}^{1} \mathrm{d}x_L D(x_L), \qquad \langle D\rangle_{\theta_R} = \delta \int_{x_c}^{1} \mathrm{d}x_L \frac{x_L\, D(x_L)}{\sqrt{x_L^2 \pm x_{cr}^2}}, \tag{28}$$

$$\langle x_L D\rangle_{\theta_L} = \int_{x_c}^{1} \mathrm{d}x_L D(x_L) x_L,$$

$$\langle x_L I_L\rangle_{\theta_L} = \int_{x_c}^{1} \frac{x_L D(x_L)\,\mathrm{d}x_L}{\sqrt{1+(kl_L)^2\left(1-x_L^2\right)}}, \qquad \langle x_L I_R\rangle_{\theta_L} = \int_{x_c}^{1} \frac{x_L D(x_L)\mathrm{d}x_L}{\sqrt{1+(kl_R\delta)^2\left(1-x_L^2\right)}}, \tag{29}$$

$$\widetilde{\lambda}_1 = \int_{x_c}^{1} \mathrm{d}x_L \frac{D(x_L)}{\sqrt{1+(kl_L)^2\left(1-x_L^2\right)}}, \tag{30}$$

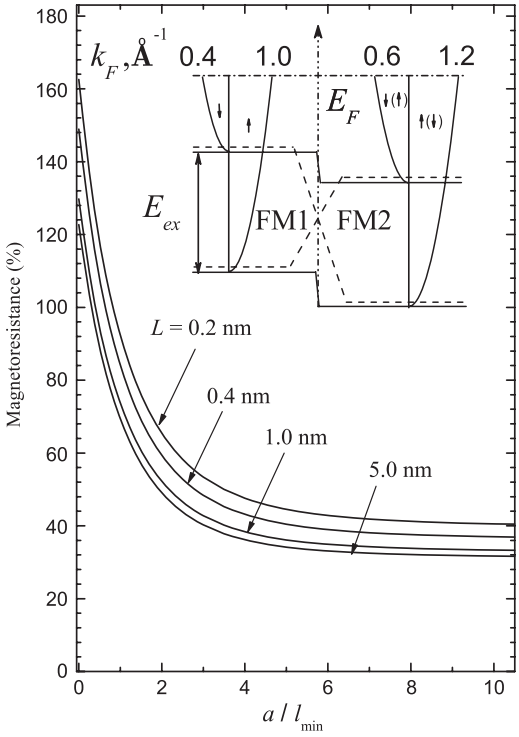

Figure 2. Dependence of MR on the contact size for the case $k_{FL\downarrow} < k_{FR\downarrow} < k_{FL\uparrow} < k_{FR\uparrow}$. The layout and choice of the mean free paths are the same as in figure 1.

$$\widetilde{\lambda}_2 = \int_{x_c}^{1} \mathrm{d}x_L \frac{\delta\, x_L\, D(x_L)}{\sqrt{x_L^2 \pm x_{cr}^2}\sqrt{1 + (kl_R\delta)^2\left(1 - x_L^2\right)}}, \tag{31}$$

$$\widetilde{\lambda}_3 = \int_{x_c}^{1} \mathrm{d}x_L \frac{\delta\, x_L\, D(x_L)}{\sqrt{x_L^2 \pm x_{cr}^2}\sqrt{1 + (kl_L)^2\left(1 - x_L^2\right)}}, \tag{32}$$

$$\widetilde{\lambda}_4 = \int_{x_c}^{1} \mathrm{d}x_L \frac{D(x_L)}{\sqrt{1 + (kl_R\delta)^2\left(1 - x_L^2\right)}}, \tag{33}$$

where $\delta = k_{FL}/k_{FR}$. If $k_{FL} < k_{FR}$, then $x_c = 0$, $x_{cr} = \sqrt{(1-\delta^2)\delta^2}$, and the upper sign in the square roots has to be used. When $k_{FL} > k_{FR}$, then $x_c = x_{cr}$, $x_{cr} = \sqrt{1 - (\delta)^{-2}}$, and the lower sign in the square roots has to be used.

Figure 1 displays MR of a hypothetical heterocontact in which the right-hand side ferromagnet has larger Fermi momenta for both conduction spin-subbands compared with those for the left-hand side ferromagnet ($k_{FL\downarrow} < k_{FL\uparrow} < k_{FR\downarrow} < k_{FR\uparrow}$). In contrast to the case of a homocontact, the MR of this type of heterocontact is negative, and it decreases in absolute value when approaching the ballistic regime ($a < l_{min}$, where $l_{min} l_{L\uparrow}$, and also for figures 2 and 3). Moreover, there is a shallow valley in the range $a/l_{min} \approx$ 1–6. Positive physical magnetoresistance (to which the negative MR values are given in figure 1 because of the definition, equation (25)) is explained by sharper potential barriers (a more resistive interface) in the P alignment compared with the smoother potential landscape in the presence

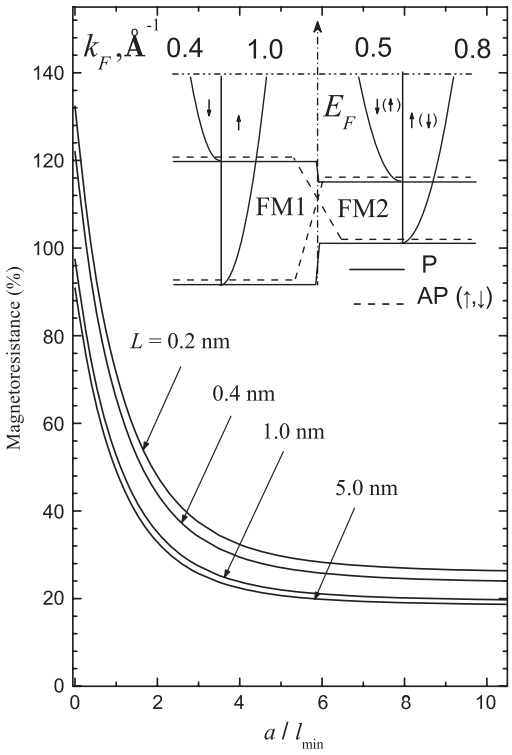

Figure 3. Dependence of MR on the contact size for the case $k_{FL\downarrow} < k_{FR\downarrow} < k_{FL\uparrow} < k_{FR\uparrow}$. The layout and choice of the mean free paths are the same as in figure 1.

of a domain wall (see the inset in figure 1). The magnitude of the magnetoresistance effect is rather small.

Magnetoresistance of the second type of heterocontact ($k_{FL\downarrow} < k_{FR\downarrow} < k_{FL\uparrow} < k_{FR\uparrow}$) is displayed in figure 2. MR is positive in the entire range of contact sizes and much bigger in magnitude compared with the first case given in figure 1. It increases by about four times upon changing the conductance regime on the size of the nanocontact from diffusive to ballistic.

Figure 3 shows the dependence of MR on the contact size for case 3 ($k_{FL\downarrow} < k_{FR\downarrow} < k_{FR\uparrow} < k_{FL\uparrow}$). The MR behaviour is similar to the second case; the sign of MR is always positive (magnetoresistance is negative). A considerable enhancement of MR follows from the calculations upon approaching the ballistic regime of conductance in the vicinity of the nanocontact. It is worth noting here that if we exchange spin indices of all spin-dependent quantities in the formulas above, then the MR(a) dependences in figures 1–3 do not change.

3.3. Discussion of experiments

To the authors' knowledge there are three reports on magnetoresistance measurements in ferromagnetic heterocontacts: Mumetal–Ni [23, 24] and CrO_2–Ni [25]. Mumetal ($Ni_{77}Fe_{14}Cu_5Mo_4$) is close to Permalloy ($Ni_{79}Fe_{21}$) in its composition. Therefore, we may use the material parameters of Permalloy and nickel [16, 26–32] as a trial guess to calculate the MR of the Mumetal–Ni couple. The results for MR are displayed in figure 4; the parameters that we used for the calculations correspond to case 3 (figure 3), and are given in the figure.

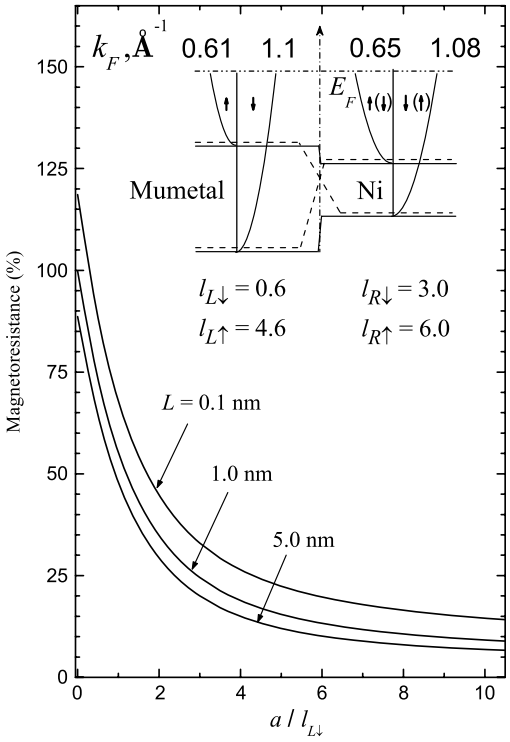

Figure 4. Dependence of MR on the contact size for the choice of parameters close to the Mumetal–Ni heterocontact. The values of parameters are given in the figure.

The ballistic limit magnitude of MR varies in the range 88–120% ($L = 0.1$–5 nm), which agrees satisfactorily with the experimental values of MR = 78–132% quoted in table 1 of [23] and figure 2 in [24] at the smallest conductances for the P-alignment of magnetizations. As for the case of a CrO_2–Ni heterocontact [25], we would abstain from considering the data in the frame of the present calculations, because the parallel alignment conductance is too low to treat the Ni–CrO_2 nanocontacts as being true metallic conducting ones. The tunnelling conductance regime, which we suspect in Ni–CrO_2 heterocontacts, is beyond the scope of our theory.

4. Conclusions

To summarize, in this paper we investigated GMR theoretically in nanoscale ferromagnetic heterocontacts. The quasi-classical theory of magnetic nanocontacts was generalized for the case of metallic ferromagnets with arbitrary Fermi momenta and mean free paths of the conduction spin-subbands. The heterocontacts were sorted by three types of mutual positions of conduction spin-subband bottoms. A model of the linear domain wall profile for an antiparallel alignment of magnetizations in contacting ferromagnets was used to account for the finite contact length. In general, the magnetoresistance plotted against the size of the nanocontact can be of either sign, depending on the conduction bands matching. The magnitude of the effect for heterocontacts in our calculations was always smaller than that for a contact made of the same ferromagnetic metal. The magnetoresistance in the case when one of the ferromagnetic metals has both Fermi momenta of the conduction electron spin-subbands smaller than the other is

always much smaller compared with the other band arrangements considered in the paper. The theoretical results agree satisfactorily with the available experimental data on the ferromagnetic heterocontacts Mumetal–Ni.

Acknowledgments

Stimulating conversations with Professor N García are gratefully acknowledged. The work was supported by the European Commission grant NMP4-CT-2003-505282.

References

[1] García N, Muñoz M and Zhao Y-W 1999 *Phys. Rev. Lett.* **82** 2923
[2] Tatara G, Zhao Y-W, Muñoz M and García N 1999 *Phys. Rev. Lett.* **83** 2030
[3] García N, Muñoz M and Zhao Y-W 2000 *Appl. Phys. Lett.* **76** 2586
[4] Zhao Y-W, Muñoz M, Tatara G and García N 2001 *J. Magn. Magn. Mater.* **223** 169
[5] García N, Muñoz M, Qian G G, Rohrer H, Saveliev I G and Zhao Y-W 2001 *Appl. Phys. Lett.* **79** 4550
[6] García N, Muñoz M, Osipov V V, Ponizovskaya E V, Qian G G, Saveliev I G and Zhao Y-W 2002 *J. Magn. Magn. Mater.* **240** 92
[7] Sullivan M R, Boehm D A, Ateya D A, Hua S Z and Chopra H D 2005 *Phys. Rev.* B **71** 024412
[8] Chopra H D, Sullivan M R, Armstrong J N and Hua S Z 2005 *Nat. Mater.* **4** 832
[9] Imamura H, Kobayashi N, Takahashi S and Maekawa S 2000 *Phys. Rev. Lett.* **84** 1003
[10] Zvezdin A K and Popkov A F 2000 *Pis. Zh. Eksp. Teor. Fiz.* **71** 304
Zvezdin A K and Popkov A F 2000 *JETP Lett.* **71** 209 (Engl. Transl.)
[11] Tagirov L R, Vodopyanov B P and Efetov K B 2001 *Phys. Rev.* B **63** 104468
[12] Bruno P 1999 *Phys. Rev. Lett.* **83** 2425
[13] Savchenko L L, Zvezdin A K, Popkov A F and Zvezdin K A 2001 *Fiz. Tverd. Tela* **43** 1449
Savchenko L L, Zvezdin A K, Popkov A F and Zvezdin K A 2001 *Phys. Solid State* **43** 1509 (Engl. Transl.)
[14] Molyneux V A, Osipov V V and Ponizovskaya E V 2002 *Phys. Rev.* B **65** 184425
[15] Labaye Y, Berger L and Coey J M D 2002 *J. Appl. Phys.* **91** 5341
[16] Dieny B J 1994 *J. Magn. Magn. Mater.* **136** 335
[17] Zaitsev A V 1984 *Zh. Eksp. Teor. Fiz.* **86** 1742
Zaitsev A V 1984 *Sov. Phys.—JETP* **59** 1015 (Engl. Transl.)
[18] Tagirov L R, Vodopyanov B P and Efetov K B 2002 *Phys. Rev.* B **65** 214419
[19] Gopar V A, Weinmann D, Jalabert R A and Stamps R L 2004 *Phys. Rev.* B **69** 014426
[20] Kazantseva N, Wieser R and Nowak U 2005 *Phys. Rev. Lett.* **94** 037206
[21] Stearns M B 1977 *J. Magn. Magn. Mater.* **5** 167
Stearns M B 1993 *J. Appl. Phys.* **73** 6396
[22] Jansen R and Lodder J C 2000 *Phys. Rev.* B **61** 5860
[23] García N, Zhao Y-W, Muñoz M and Saveliev I G 2000 *IEEE Trans. Magn.* **36** 2833
[24] Zhao Y-W, Muñoz M, Tatara G and García N 2001 *J. Magn. Magn. Mater.* **223** 169
[25] Chung S H, Muñoz M, García N, Egelhoff W F Jr and Gomez R D 2002 *Phys. Rev. Lett.* **89** 287203
[26] Gurney B A, Speriosu V S, Nozieres J-P, Lefakis H, Wilhoit D R and Need O U 1993 *Phys. Rev. Lett.* **71** 4023
[27] Petrovykh D Y, Altmann K N, Höchst H, Laubscher M, Maat S, Mankey G J and Himpsel F J 1998 *Appl. Phys. Lett.* **73** 3459
[28] Himpsel F J, Ortega J E, Mankey G J and Willis R F 1998 *Adv. Phys.* **47** 511
[29] Himpsel F J, Altmann K N, Mankey G J, Ortega J E and Petrovykh D Y 1999 *J. Magn. Magn. Mater.* **200** 456
[30] Himpsel F J 1999 *J. Phys.: Condens. Matter* **11** 9483
[31] Altmann K N, Petrovykh D Y, Mankey G J, Shannon N, Gilman N, Hochstrasser M, Willis R F and Himpsel F J 2000 *Phys. Rev.* B **61** 15661
[32] Altmann K N, Gilman N, Hayoz J, Willis R F and Himpsel F J 2001 *Phys. Rev. Lett.* **87** 137201